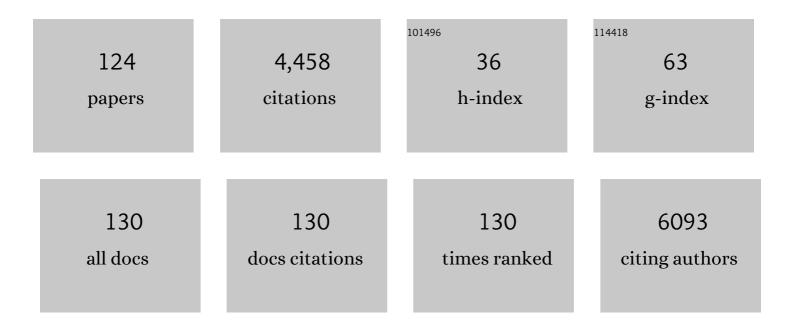
List of Publications by Year in descending order

Source: https://exaly.com/author-pdf/6088645/publications.pdf Version: 2024-02-01



#	Article	IF	CITATIONS
1	Atomistic mechanisms underlying plasticity and crack growth in ceramics: a case study of AlN/TiN superlattices. Acta Materialia, 2022, 229, 117809.	3.8	29
2	Ca Solubility in a BiFeO <sub>3</sub> -Based System with a Secondary Bi <sub>2</sub> O <sub>3</sub> Phase on a Nanoscale. Journal of Physical Chemistry C, 2022, 126, 7696-7703.	1.5	1
3	Atomic-scale understanding of the structural evolution in TiN/AlN superlattice during nanoindentation—Part 2: Strengthening. Acta Materialia, 2022, 234, 118009.	3.8	3
4	Atomic-scale understanding of the structural evolution of TiN/AlN superlattice during nanoindentation— Part 1: Deformation. Acta Materialia, 2022, 234, 118008.	3.8	6
5	Fracture toughness trends of modulus-matched TiN/(Cr,Al)N thin film superlattices. Acta Materialia, 2021, 202, 376-386.	3.8	35
6	Real-time atomic-resolution observation of coherent twin boundary migration in CrN. Acta Materialia, 2021, 208, 116732.	3.8	10
7	Atomic insights on intermixing of nanoscale nitride multilayer triggered by nanoindentation. Acta Materialia, 2021, 214, 117004.	3.8	19
8	Correlating point defects with mechanical properties in nanocrystalline TiN thin films. Materials and Design, 2021, 207, 109844.	3.3	18
9	Negatively Charged In-Plane and Out-Of-Plane Domain Walls with Oxygen-Vacancy Agglomerations in a Ca-Doped Bismuth-Ferrite Thin Film. ACS Applied Electronic Materials, 2021, 3, 4498-4508.	2.0	4
10	The formation of TiO <sub>2</sub> /VO <sub>2</sub> multilayer structure <i>via</i> directional cationic diffusion. Nanoscale, 2021, 13, 7783-7791.	2.8	10
11	Combined Fe and O effects on microstructural evolution and strengthening in Cu–Fe nanocrystalline alloys. Materials Science & Engineering A: Structural Materials: Properties, Microstructure and Processing, 2020, 772, 138800.	2.6	16
12	Growth-twins in CrN/AlN multilayers induced by hetero-phase interfaces. Acta Materialia, 2020, 185, 157-170.	3.8	8
13	PLD growth and characteristics of lead-free NKLNST ferroelectric nanotubes. Journal of Materials Research and Technology, 2020, 9, 12818-12823.	2.6	1
14	Strain-induced structure and oxygen transport interactions in epitaxial La0.6Sr0.4CoO3â^î^ thin films. Communications Materials, 2020, 1, .	2.9	8
15	Indentation response of a superlattice thin film revealed by in-situ scanning X-ray nanodiffraction. Acta Materialia, 2020, 195, 425-432.	3.8	7
16	Atomic-scale study on incoherent twin boundary evolution in nanograined Cu. Scripta Materialia, 2020, 186, 278-281.	2.6	7
17	Fracture properties of thin film TiN at elevated temperatures. Materials and Design, 2020, 194, 108885.	3.3	36
18	Study on Ca Segregation toward an Epitaxial Interface between Bismuth Ferrite and Strontium Titanate. ACS Applied Materials & Interfaces, 2020, 12, 12264-12274.	4.0	5

#	Article	IF	CITATIONS
19	Atomic-scale investigation on the structural evolution and deformation behaviors of Cu–Cr nanocrystalline alloys processed by high-pressure torsion. Journal of Alloys and Compounds, 2020, 832, 154994.	2.8	4
20	Mapping the mechanical properties in nitride coatings at the nanometer scale. Acta Materialia, 2020, 194, 343-353.	3.8	6
21	Mechanical properties and epitaxial growth of TiN/AlN superlattices. Surface and Coatings Technology, 2019, 375, 1-7.	2.2	25
22	Atomic resolution analyses on defects in nanocrystalline Cu-based alloys generated by severe plastic deformation. Materials Characterization, 2019, 157, 109886.	1.9	3
23	Direct atomic identification of cation migration induced gradual cubic-to-hexagonal phase transition in Ge2Sb2Te5. Communications Chemistry, 2019, 2, .	2.0	32
24	Correlating elemental distribution with mechanical properties of TiN/SiNx nanocomposite coatings. Scripta Materialia, 2019, 170, 20-23.	2.6	23
25	Toughness enhancement in TiN/WN superlattice thin films. Acta Materialia, 2019, 172, 18-29.	3.8	72
26	Correlating structural and mechanical properties of AlN/TiN superlattice films. Scripta Materialia, 2019, 165, 159-163.	2.6	29
27	The Route to Supercurrent Transparent Ferromagnetic Barriers in Superconducting Matrix. ACS Nano, 2019, 13, 5655-5661.	7.3	4
28	Crystallographic orientation dependent maximum layer thickness of cubic AlN in CrN/AlN multilayers. Acta Materialia, 2019, 168, 190-202.	3.8	31
29	Tracking the Structural and Chemical Evolution of Nanostructured Materials by In-Situ Experiments. Microscopy and Microanalysis, 2019, 25, 19-20.	0.2	0
30	Oxygen-mediated deformation and grain refinement in Cu-Fe nanocrystalline alloys. Acta Materialia, 2019, 166, 281-293.	3.8	37
31	On the stacking fault energy related deformation mechanism of nanocrystalline Cu and Cu alloys: A first-principles and TEM study. Journal of Alloys and Compounds, 2019, 776, 807-818.	2.8	36
32	Graphene-templated synthesis of palladium nanoplates as novel electrocatalyst for direct methanol fuel cell. Applied Surface Science, 2019, 466, 385-392.	3.1	106
33	In situ atomic-scale observation of oxidation and decomposition processes in nanocrystalline alloys. Nature Communications, 2018, 9, 946.	5.8	14
34	Origin of large plasticity and multiscale effects in iron-based metallic glasses. Nature Communications, 2018, 9, 1333.	5.8	89
35	Fracture toughness of Ti-Si-N thin films. International Journal of Refractory Metals and Hard Materials, 2018, 72, 78-82.	1.7	40
36	Insight into the structural evolution during TiN film growth via atomic resolution TEM. Journal of Alloys and Compounds, 2018, 754, 257-267.	2.8	36

#	Article	IF	CITATIONS
37	Novel synthesis of core-shell Au-Pt dendritic nanoparticles supported on carbon black for enhanced methanol electro-oxidation. Applied Surface Science, 2018, 433, 840-846.	3.1	39
38	Ultrafast Giant Photostriction of Epitaxial Strontium Iridate Film with Superior Endurance. Nano Letters, 2018, 18, 7742-7748.	4.5	21
39	High electrocatalytic performance of a graphene-supported PtAu nanoalloy for methanolÂoxidation. International Journal of Hydrogen Energy, 2018, 43, 12803-12810.	3.8	37
40	Microstructural and texture evolution of copper-(chromium, molybdenum, tungsten) composites deformed by high-pressure-torsion. International Journal of Refractory Metals and Hard Materials, 2018, 75, 137-146.	1.7	6
41	Influence of phase transformation on the damage tolerance of Ti-Al-N coatings. Vacuum, 2018, 155, 153-157.	1.6	15
42	Complementary High Spatial Resolution Methods in Materials Science and Engineering. Advanced Engineering Materials, 2017, 19, 1600671.	1.6	5
43	On the phase evolution and dissolution process in Cu-Cr alloys deformed by high pressure torsion. Scripta Materialia, 2017, 133, 41-44.	2.6	26
44	Pt nanoparticles modified Au dendritic nanostructures: Facile synthesis and enhanced electrocatalytic performance for methanol oxidation. International Journal of Hydrogen Energy, 2017, 42, 22100-22107.	3.8	22
45	Revealing the Microstructural evolution in Cu-Cr nanocrystalline alloys during high pressure torsion. Materials Science & Engineering A: Structural Materials: Properties, Microstructure and Processing, 2017, 695, 350-359.	2.6	16
46	On nanostructured molybdenum–copper composites produced by high-pressure torsion. Journal of Materials Science, 2017, 52, 9872-9883.	1.7	12
47	In-situ tracking the structural and chemical evolution of nanostructured CuCr alloys. Acta Materialia, 2017, 138, 42-51.	3.8	17
48	Dislocation densities and alternating strain fields in CrN/AlN nanolayers. Thin Solid Films, 2017, 638, 189-200.	0.8	19
49	Fracture toughness and structural evolution in the TiAlN system upon annealing. Scientific Reports, 2017, 7, 16476.	1.6	93
50	Superlattice-induced oscillations of interplanar distances and strain effects in the CrN/AlN system. Physical Review B, 2017, 95, .	1.1	13
51	Transmission electron microscopical study of teenage crown dentin on the nanometer scale. Materials Science and Engineering C, 2017, 71, 994-998.	3.8	5
52	Orientation of FePt nanoparticles on top of a-SiO <sub>2</sub> /Si(001), MgO(001) and sapphire(0001): effect of thermal treatments and influence of substrate and particle size. Beilstein Journal of Nanotechnology, 2016, 7, 591-604.	1.5	5
53	Crossover between superconductivity and magnetism in SrRuO <sub>3</sub> mesocrystal embedded YBa <sub>2</sub> Cu <sub>3</sub> O <sub>7â^'x</sub> heterostructures. Nanoscale, 2016, 8, 18454-18460.	2.8	3
54	Highâ€Performance Smallâ€Amount Fe <sub>2</sub> O <sub>3</sub> â€Doped (K,Na)NbO <sub>3</sub> â€Based Leadâ€Free Piezoceramics with Irregular Phase Evolution. Journal of the American Ceramic Society, 2016, 99, 2341-2346.	1.9	38

#	Article	IF	CITATIONS
55	Giant heterogeneous magnetostriction in Fe–Ga alloys: Effect of trace element doping. Acta Materialia, 2016, 109, 177-186.	3.8	112
56	Microstructure characterization of Al–Cr–Fe quasicrystals sintered using spark plasma sintering. Materials Characterization, 2015, 110, 264-271.	1.9	16
57	Study on the Atomic and Electronic Structure in CrN (VN, TiN) Films using CS-Corrected TEM. Microscopy and Microanalysis, 2015, 21, 2079-2080.	0.2	0
58	Controllable synthesis of palladium nanocubes/reduced graphene oxide composites and their enhanced electrocatalytic performance. Journal of Power Sources, 2015, 280, 422-429.	4.0	25
59	Nitrogen atom shift and the structural change in chromium nitride. Acta Materialia, 2015, 98, 119-127.	3.8	6
60	The peculiarity of the metal-ceramic interface. Scientific Reports, 2015, 5, 11460.	1.6	22
61	Microstructural evolution and grain refinement in an intermetallic titanium aluminide alloy with a high molybdenum content. International Journal of Materials Research, 2015, 106, 725-731.	0.1	18
62	An Epitaxial Ferroelectric Tunnel Junction on Silicon. Advanced Materials, 2014, 26, 7185-7189.	11.1	61
63	New insights on the formation of supersaturated solid solutions in the Cu–Cr system deformed by high-pressure torsion. Acta Materialia, 2014, 69, 301-313.	3.8	73
64	Evolution of the ωo phase in a β-stabilized multi-phase TiAl alloy and its effect on hardness. Acta Materialia, 2014, 64, 241-252.	3.8	144
65	Revealing the atomic and electronic structure of a SrTiO3/LaNiO3/SrTiO3 heterostructure interface. Journal of Applied Physics, 2014, 115, 103519.	1.1	7
66	Insights into the atomic and electronic structure triggered by ordered nitrogen vacancies in CrN. Physical Review B, 2013, 87, .	1.1	22
67	Transmission electron microscopy characterization of CrN films on MgO(001). Thin Solid Films, 2013, 545, 154-160.	0.8	3
68	Current Oscillations in the Layer-by-Layer Electrochemical Deposition of Vertically Aligned Nanosheets of Zinc Hydroxide Nitrate. Journal of the Electrochemical Society, 2013, 160, D558-D564.	1.3	7
69	Advanced nanomechanics in the TEM: effects of thermal annealing on FIB prepared Cu samples. Philosophical Magazine, 2012, 92, 3269-3289.	0.7	48
70	Local symmetry breaking of a thin crystal structure of Â-Si3N4 as revealed by spherical aberration corrected high-resolution transmission electron microscopy images. Journal of Electron Microscopy, 2012, 61, 145-57.	0.9	1
71	Lateral gradients of phases, residual stress and hardness in a laser heated Ti0.52Al0.48N coating on hard metal. Surface and Coatings Technology, 2012, 206, 4502-4510.	2.2	37
72	Influence of interrupted quenching on artificial aging of Al–Mg–Si alloys. Acta Materialia, 2012, 60, 4496-4505.	3.8	71

#	Article	IF	CITATIONS
73	In Situ Study of γâ€TiAl Lamellae Formation in Supersaturated α <sub>2</sub> â€Ti <sub>3</sub> Al Grains. Advanced Engineering Materials, 2012, 14, 299-303.	1.6	12
74	Deformation mechanisms of a modified 316L austenitic steel subjected to high pressure torsion. Materials Science & Engineering A: Structural Materials: Properties, Microstructure and Processing, 2011, 528, 2776-2786.	2.6	95
75	Electrical properties and structure of grain boundaries in n-conducting BaTiO3 ceramics. Journal of the European Ceramic Society, 2011, 31, 763-771.	2.8	21
76	Dynamic behavior of nanometer-scale amorphous intergranular film in silicon nitride by in situ high-resolution transmission electron microscopy. Journal of the European Ceramic Society, 2011, 31, 1835-1840.	2.8	3
77	Atomic and electronic structures of a transition layer at the CrN/Cr interface. Journal of Applied Physics, 2011, 110, 043524.	1.1	5
78	Structural characterization of a Cu/MgO(001) interface using CS-corrected HRTEM. Thin Solid Films, 2010, 519, 1662-1667.	0.8	26
79	Large-Scale Synthesis of SnO <sub>2</sub> Nanosheets with High Lithium Storage Capacity. Journal of the American Chemical Society, 2010, 132, 46-47.	6.6	626
80	Unveiling the atomic and electronic structure of the VN/MgO interface. Physical Review B, 2010, 82, .	1.1	3
81	Magnetic properties and atomic structure of La2/3Ca1/3MnO3–YBa2Cu3O7 heterointerfaces. Applied Physics Letters, 2009, 95, .	1.5	25
82	Homogeneity of the superplastic Zr <sub>64.13</sub> Cu <sub>15.75</sub> Ni <sub>10.12</sub> Al <sub>10</sub> bulk metallic glass. Journal of Materials Research, 2009, 24, 3116-3120.	1.2	11
83	Behaviour of TEM metal grids during in-situ heating experiments. Ultramicroscopy, 2009, 109, 766-774.	0.8	44
84	Interfacial microstructure and defect analysis in Cu(In,Ga)Se([sub]2)-based multilayered film by analytical transmission electron microscopy and focused ion beam. Thin Solid Films, 2009, 517, 4329-4335.	0.8	2
85	Structural imaging of $\hat{l}^2$ -Si3N4 by spherical aberration-corrected high-resolution transmission electron microscopy. Ultramicroscopy, 2009, 109, 1114-1120.	0.8	15
86	Synthesis, Thermal Stability and Properties of ZnO <sub>2</sub> Nanoparticles. Journal of Physical Chemistry C, 2009, 113, 1320-1324.	1.5	79
87	Anomalous compressive behavior in CeO <sub>2</sub> nanocubes under high pressure. New Journal of Physics, 2008, 10, 123016.	1.2	19
88	Single-Phase Titania Nanocrystallites and Nanofibers from Titanium Tetrachloride in Acetone and Other Ketones. Inorganic Chemistry, 2007, 46, 5093-5099.	1.9	29
89	Microstructure characterization of a cobalt-oxide-doped cerium-gadolinium-oxide by analytical and high-resolution TEM. Acta Materialia, 2007, 55, 2907-2917.	3.8	37
90	Surface effects in the energy loss near edge structure of different cobalt oxides. Ultramicroscopy, 2007, 107, 598-603.	0.8	38

#	Article	IF	CITATIONS
91	Thin tantalum–silicon–oxygen/tantalum–silicon–nitrogen films as high-efficiency humidity diffusion barriers for solar cell encapsulation. Thin Solid Films, 2006, 515, 1612-1617.	0.8	11
92	Microstructure of cobalt oxide doped sintered ceria solid solutions. Journal of Electroceramics, 2006, 16, 191-197.	0.8	42
93	Electron energy-loss spectroscopy study of a multilayered SiOx and SiOxCy film prepared by plasma-enhanced chemical vapor deposition. Journal of Materials Research, 2006, 21, 608-612.	1.2	5
94	Comparative studies of microstructure and impedance of small-angle symmetrical and asymmetrical grain boundaries in SrTiO3. Acta Materialia, 2005, 53, 5007-5015.	3.8	49
95	Schottky barrier formed by network of screw dislocations in SrTiO3. Applied Physics Letters, 2005, 87, 162105.	1.5	22
96	Electrical resistance of low-angle tilt grain boundaries in acceptor-doped SrTiO3 as a function of misorientation angle. Journal of Applied Physics, 2005, 97, 053502.	1.1	63
97	HRTEM and EELS study of screw dislocation cores inSrTiO3. Physical Review B, 2004, 69, .	1.1	37
98	Growth of compound single- and multi-walled carbon nanotubes. Ultramicroscopy, 2004, 98, 195-200.	0.8	2
99	A simple method to synthesise single-crystalline manganese oxide nanowires. Chemical Physics Letters, 2003, 378, 349-353.	1.2	133
100	Electrical and Structural Characterization of a Lowâ€Angle Tilt Grain Boundary in Ironâ€Đoped Strontium Titanate. Journal of the American Ceramic Society, 2003, 86, 922-928.	1.9	103
101	Grain size dependent grain boundary defect structure: case of doped zirconia. Acta Materialia, 2003, 51, 2539-2547.	3.8	170
102	High-concentration nitrogen-doped carbon nanotube arrays. Nanotechnology, 2003, 14, 931-934.	1.3	30
103	Uniformly distributed nickel nanoparticles created by heating the carbon nanotube. Journal of Materials Research, 2003, 18, 604-608.	1.2	1
104	Direct Atom-Resolved Imaging of Oxides and Their Grain Boundaries. Science, 2003, 302, 846-849.	6.0	88
105	Irradiation-induced dissociation of anaâŸ <sup></sup> 100⟩ edge dislocation in SrTiO3. Philosophical Magazine Letters, 2003, 83, 711-719.	0.5	3
106	Compound growth and microstructure of carbon nanotube. Journal of Materials Research, 2003, 18, 2459-2463.	1.2	1
107	Atomic and electronic characterization of thea[100]dislocation core inSrTiO3. Physical Review B, 2002, 66, .	1.1	108
108	Electronic and atomic structure of a dissociated dislocation inSrTiO3. Physical Review B, 2002, 66, .	1.1	93

#	Article	IF	CITATIONS
109	Synthesis and Microstructure of Antimony Oxide Nanorods. Journal of Materials Research, 2002, 17, 1698-1701.	1.2	12
110	Comprehensive characterization of iron oxide containing mesoporous molecular sieve MCM-41. Studies in Surface Science and Catalysis, 2002, , 403-410.	1.5	8
111	Structure and Chemical Transformation in Cerium Oxide Nanoparticles Coated by Surfactant Cetyltrimethylammonium Bromide (CTAB):Â An X-ray Absorption Spectroscopic Study. Journal of Physical Chemistry B, 2002, 106, 4569-4577.	1.2	53
112	Structural Characteristics of Cerium Oxide Nanocrystals Prepared by the Microemulsion Method. Chemistry of Materials, 2001, 13, 4192-4197.	3.2	116
113	Vanadium- and chromium-containing mesoporous MCM-41 molecular sieves with hierarchical structure. Microporous and Mesoporous Materials, 2001, 43, 227-236.	2.2	20
114	Morphogenesis of surface patterns and incorporation of redox-active metals in mesoporous silicate molecular sieves. Surface and Interface Analysis, 2001, 32, 193-197.	0.8	11
115	Synthesis and characterization of antimony oxide nanoparticles. Journal of Materials Research, 2001, 16, 803-805.	1.2	46
116	Grain boundary segregation in ultra-low carbon steel. Materials Science & Engineering A: Structural Materials: Properties, Microstructure and Processing, 2000, 291, 22-26.	2.6	35
117	Characterization of the microstructure of Co thin film on silicon substrate by TEM. Journal of Electronic Materials, 2000, 29, 617-621.	1.0	0
118	Non-equilibrium intergranular segregation in ultra low carbon steel. Materials Science and Technology, 2000, 16, 305-308.	0.8	21
119	Study of the double layer CeO2/Nb2O5 thin film. Journal of Vacuum Science and Technology A: Vacuum, Surfaces and Films, 2000, 18, 2928-2931.	0.9	12
120	Stability of Carbon Nanotubes: How Small Can They Be?. Physical Review Letters, 2000, 85, 3249-3252.	2.9	142
121	Filling of single-walled carbon nanotubes with silver. Journal of Materials Research, 2000, 15, 2658-2661.	1.2	37
122	The observation of Co film oxidation on Si and SiO2 substrates. Thin Solid Films, 1996, 286, 295-298.	0.8	14
123	<i>In Situ</i> TEM Heating Study of the γ Lamellae Formation inside the α <sub>2</sub> Matrix of a Ti-45Al-7.5Nb Alloy. Advanced Materials Research, 0, 146-147, 1365-1368.	0.3	1
124	Toughness Enhancement in TiN/WN Superlattice Thin Films. SSRN Electronic Journal, 0, , .	0.4	0